Supplementary material

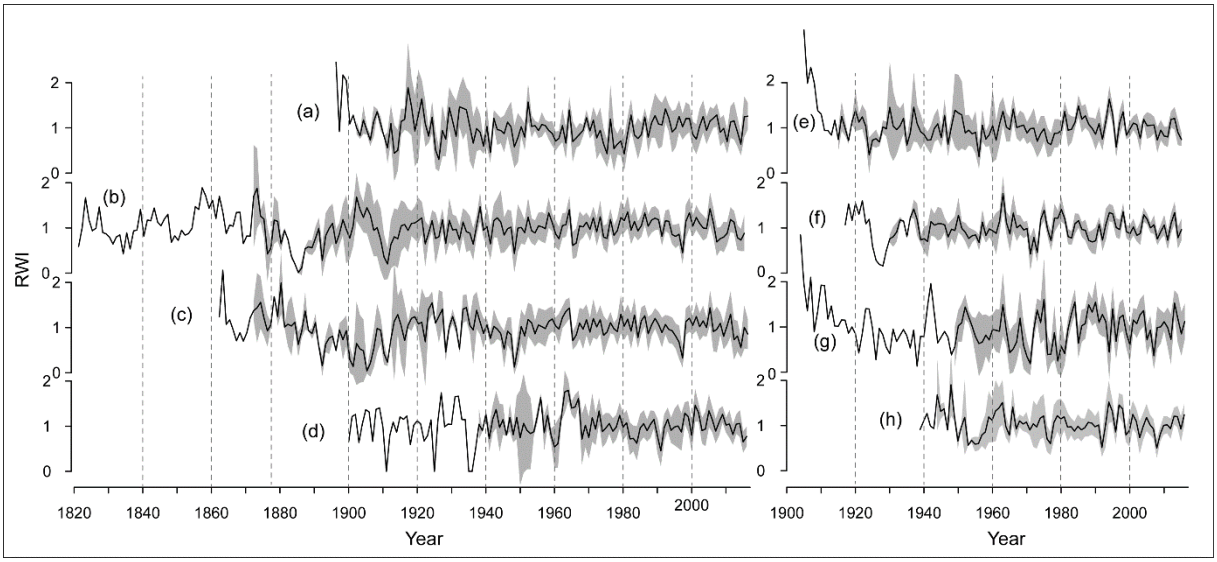

Figure S1: Detrended *R. ferrugineum* ring width (RWI) chronologies from CN2400 (a), SAL2000 (b), SAL1800 (c), CHAR (d), QGL (e), QN (f), QW (g) and LORIAZ (h) and their confidence intervals (± 1 SD; grey areas).

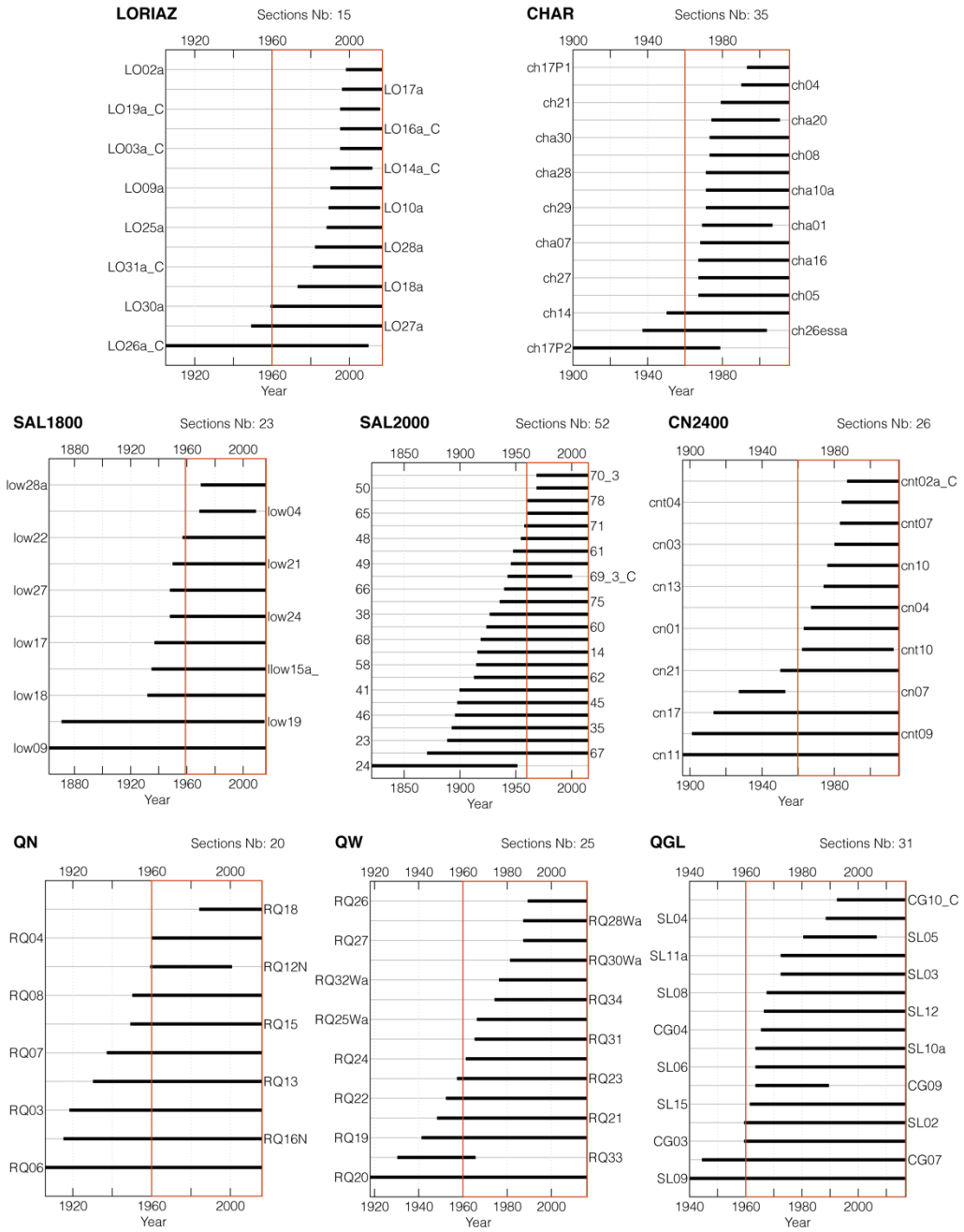

Figure S2: Sample depth of RWI chronologies (black bars) showing the number of individuals included in each chronology. Red squares correspond to the period of analysis (1960-2017). The number of section used for building chronologies is indicated above each panel.

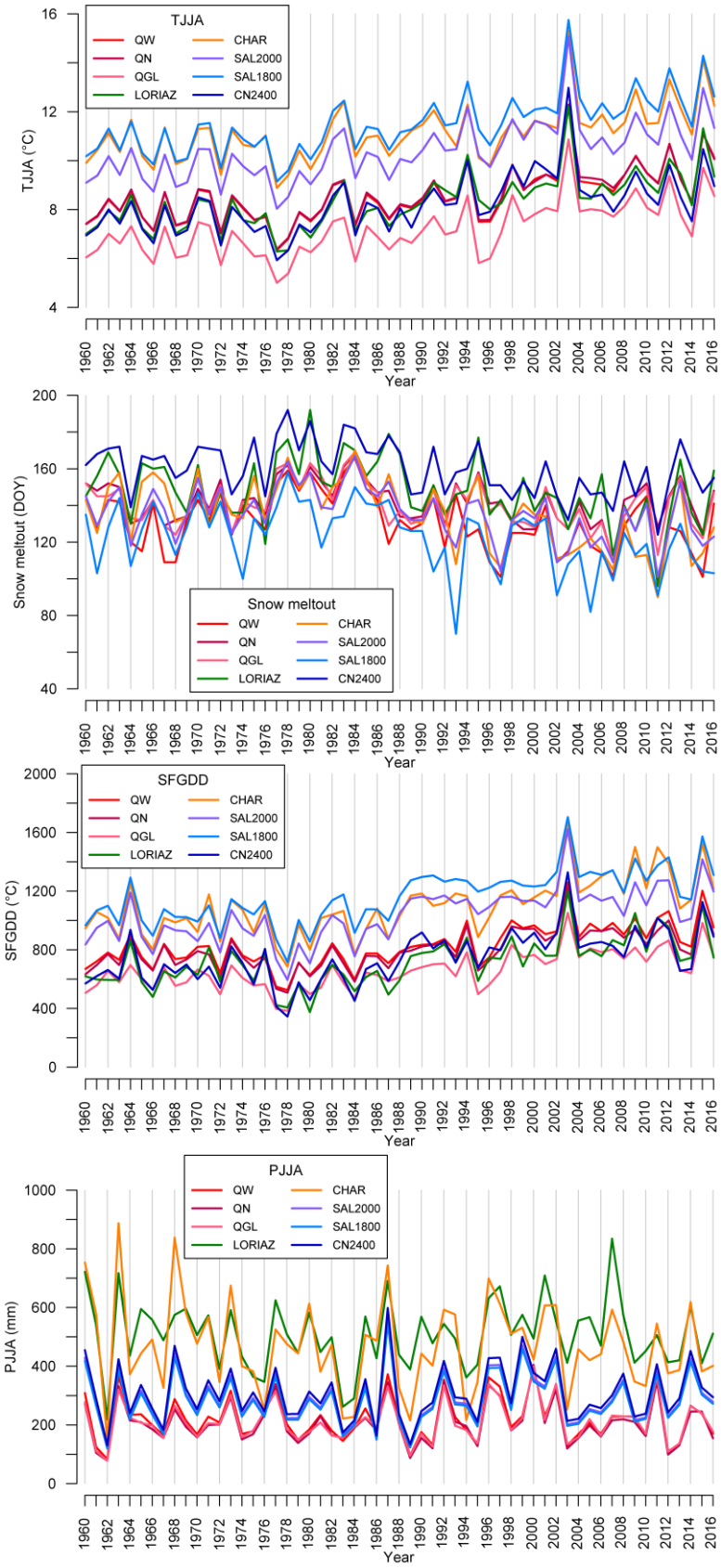

Figure S3: Trends of June-July-August mean temperature (TJJA), snow melt-out, snow-free growing degree days (SFGDD) and June-July-August precipitation sums (PJJA) at each site

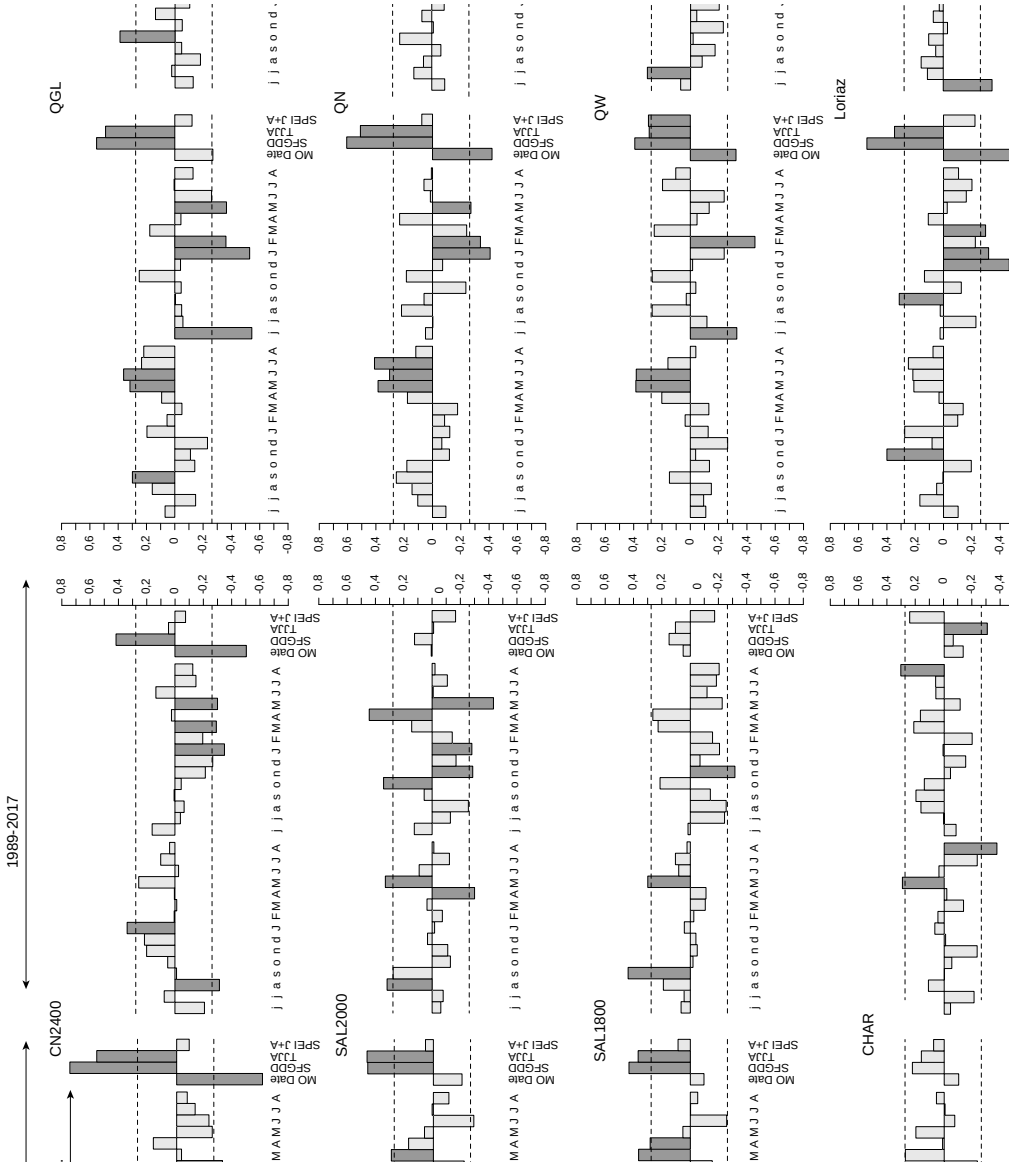

Figure S4: Bivariate correlations functions (BCFs) computed for the different sites between *R. ferrugineum* chronologies and mean temperatures (Temp.), monthly precipitation sums (Prec.), snow melt-out date (MO Date), Snow-Free Growing Degree Days (SFGDD), summer temperature (TJJA) and July-August Standardized Precipitation-Evapotranspiration Index (SPEI J+A) for the time periods 1960–1988 and 1989–2017. Months of the year preceding (N-1) ring formation (N) are written with lowercase letters; months of the current (N) year are written with capital letters. Gray-filled bars denote significant correlation at $p \leq 0.05$).

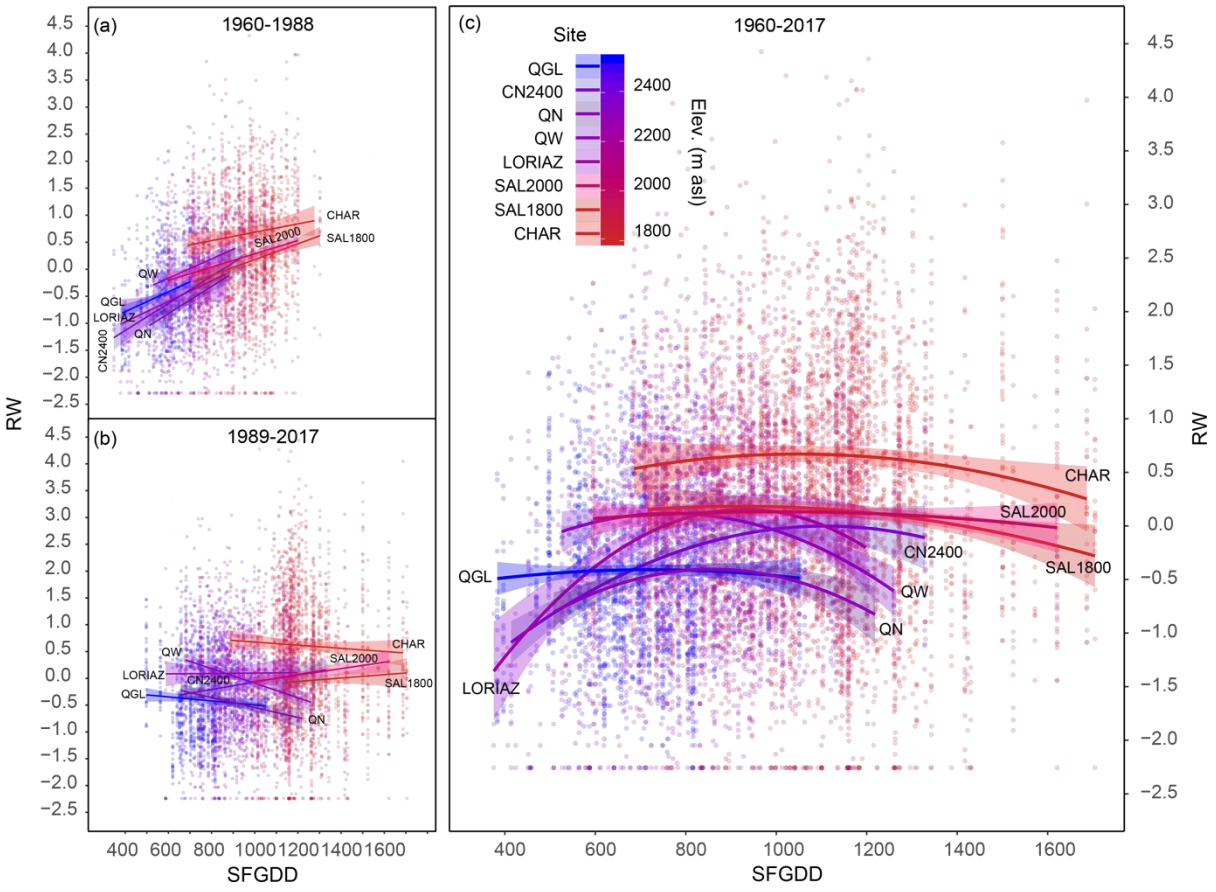

Figure S5: Relationship between snow-free growing degree days (SFGDD) and log-transformed scaled raw ring-width (RW) at each site for the 1960–1988 (a), 1989–2017 (b) and 1960-2017 periods. Regression lines with their 0.95 confidence intervals are arranged by color according to site elevation. Site names are indicated at the right or left of the regression lines.